ISSN: 0273-1177
Volume 52,
Issue 6,
15 September 2013

COSPAR
COMMITTEE ON SPACE RESEARCH

ADVANCES IN SPACE RESEARCH

ELSEVIER

Propagation of normal and faster CMEs in the interplanetary medium

A. Mujiber Rahman [a,*], A. Shanmugaraju [b,1], S. Umapathy [a,2]

[a] School of Physics, Madurai Kamaraj University, Madurai 625 021, India
[b] Department of Physics, Arul Aanandar College, Karumathur 625 514, India

Abstract

We have analyzed 101 Coronal Mass Ejection (CME) events and their associated interplanetary CMEs (ICMEs) and interplanetary (IP) shocks observed during the period 1997–2005 from the list given by Mujiber Rahman et al. (2012). The aim of the present work is to correlate the interplanetary parameters such as, the speeds of IP shocks and ICMEs, CME transit time and their relation with CME parameters near the Sun. Mainly, a group of 10 faster CME events ($V_{INT} > 2200$ km/s) are compared with a list of 91 normal events of Manoharan et al. (2004). From the distribution diagrams of CME, ICME and IP shock speeds, we note that a large number of events tends to narrow towards the ambient (i.e., background) solar wind speed ($\sim$500 km/s) in agreement with the literature. Also, we found that the IP shock speed and the average ICME speed measured at 1 AU are well correlated. In addition, the IP shock speed is found to be slightly higher than the ICME speed. While the normal events show CME travel time in the range of $\sim$40–80 h with a mean value of 65 h, the faster events have lower transit time with a mean value of 40 h. The effect of solar wind drag is studied using the correlation of CME acceleration with interplanetary (IP) acceleration and with other parameters of ICMEs. While the mean acceleration values of normal and faster CMEs in the LASCO FOV are 1 m/s², 18 m/s², they are -1.5 m/s² and -14 m/s² in the interplanetary medium, respectively. The relation between CME speed and IP acceleration for normal and faster events are found to agree with that of Lindsay et al. (1999) and Gopalswamy et al. (2001) except slight deviations for the faster events. It is also seen that the faster events with less travel time face higher negative acceleration (>-10 m/s²) in the interplanetary medium up to 1 AU.
© 2013 COSPAR. Published by Elsevier Ltd. All rights reserved.

Keywords: CMEs; ICMEs; Interplanetary shocks; Transit time

1. Introduction

Coronal Mass Ejections (CMEs) are magnetically structured plasma clouds ejected from the solar corona into the solar wind, causing severe effects on the heliosphere and Earth (Gosling, 1993). It is very important to consider the background solar wind in the study of evolution of interplanetary disturbances in the distance between Sun and Earth (Manoharan, 2006). Normal solar wind blowing past Earth has a speed of 450 km/s, but occasionally the speed increases in excess of 700 km/s. The transient nature of CMEs contrasts them from the solar wind, which is a quasi steady plasma flow. Once ejected, CMEs travel through the solar wind and interact with it, often setting up fast mode MHD shocks, which in turn accelerate charged particles to very high energies (Gopalswamy et al., 2009). The CME evolution model of Chen (1996) suggests that the Lorentz force driving CMEs is caused by the toroidal current of a flux rope, which may overcome aerodynamic drag to a distance of 0.4 AU.

After the initiation of the CMEs, many of them show only relatively small accelerations in the LASCO field of view (not higher than a few tens of m s^{-2}). This "residual"

* Corresponding author. Address: Department of Physics, Hajee Karutha Rowther Howdia College, Uthamapalayam 625 533, India. Tel.: +91 9443926682.

E-mail addresses: mujib73@gmail.com (A. Mujiber Rahman), ashanmugaraju@gmail.com (A. Shanmugaraju), umapathymku@gmail.com (S. Umapathy).
[1] Tel.: +91 9842982672.
[2] On sabbatical leave to Radio Astronomy Centre, Udhagamandalam 643 001, India. Tel.: +91 9842004967.

acceleration, at heights above two solar radii, has been studied by several authors using different statistical approaches. Wang and Sheeley (1994) already established the relationship between CME acceleration and CME speed. Large event catalogues such as compiled by Gopalswamy et al. (2009) have also been analyzed for CME acceleration and CME speed. Vršnak et al. (2004) verified that there is a relation between acceleration and velocity, suggesting that, besides a propelling force, that may be active in most events and gravity there is a contribution from aerodynamic drag. This drag leads to a small positive average acceleration for events with velocity below the solar wind velocity, and a small negative acceleration for events that exceed the solar wind velocity. CME deceleration has been studied using simulations (e.g., Cargill, 2004; Lugaz et al., 2005; Case et al., 2008; Corona-Romero and Gonzalez-Esparza, 2011) and also with the STEREO and SMEI spacecraft (Howard et al., 2007; Maloney and Gallagher, 2010; Lugaz and Roussev, 2011).

CMEs in the interplanetary medium are known as interplanetary CMEs or ICMEs for short. ICMEs are also observed in the entire heliosphere (Burlaga, 1995; Balogh, 2002). When CMEs leave the surface of the Sun, the faster ones impinge on the ambient (i.e., background) medium to form interplanetary (IP) shocks. Observations of intense shock wave disturbances near 1 AU show a direct association with CMEs from the Sun (Manoharan et al., 2004). The consequences of the shock associated with a CME at the Earth are directly linked to the energy available within the CME (Manoharan and Mujiber Rahman, 2011). The interplanetary shocks are likely to be stronger near the Sun where the driving CMEs attain their maximum speed before decelerating due to the drag force exerted by the ambient medium (see e.g., Vršnak et al., 2001; Gopalswamy et al., 2001). On the other hand, many compression waves steepen into shocks far from the Sun. For this reason, there are significantly more CME-driven shocks (and CIR shocks) at Earth than at Venus (Jian et al., 2008). In this paper, we analyze 101 CMEs to investigate the link between the travel time of the CME to 1 AU and its initial speed, final speed (also its associated shock speed) at 1 AU, and its average acceleration or deceleration in the Sun–Earth distance. We study the correlation of CME parameters (speed and acceleration) near the Sun with speeds and transit time of ICMEs and IP shocks. Our sample consists of 10 faster CMEs ($V_{INT} > 2200$ km/s) which are compared with 91 normal CMEs analyzed by Manoharan et al. (2004). This paper is organized as follows. Section 2 deals with data selection. Section 3 describes the results and discussion and in Section 4 we summarize the results of this study.

2. Data selection

In the present work, we consider a set of 101 CME events from the list given by Mujiber Rahman et al. (2012) associated with ICMEs and IP shocks observed dur-

ing the period 1997–2005. Out of 101 events, Manoharan et al. (2004) analyzed 91 CME events observed from 1997 to 2002 for studying the effect of interaction of CMEs in propagation through interplanetary medium. Mujiber Rahman et al. (2012) adds 10 fast CME events observed during 1999–2005 and studied 101 events for metric and DH type II bursts association. The 91 disc-centered normal events studied by Manoharan et al. (2004) have plane-of-sky-speed in the range of ∼100 km/s to 2400 km/s. But, the faster 10 CME events have speeds in the range of 2200 km/s to 3400 km/s. The faster 10 CME events are selected from the LASCO CME list (http://cdaw.gsfc.nasa.gov/CME_list/) according to the criteria used by Manoharan et al. (2004) and the speed of CMEs should be greater than 2200 km/s. The CME parameters used in the present study are obtained from the above references and from the online CME catalog maintained by CDAW (Coordinated Data Analysis Workshop) (Yashiro et al., 2004).

Identification and selection of IP shocks and ICMEs corresponding to the 91 CME events are already described in Manoharan et al. (2004). We have utilized the data collected by them for a different purpose of comparing the normal and faster CMEs with respect to acceleration/deceleration of CMEs and ICMEs, and travel time. Further, we have obtained the data for ICMEs and IP shocks for the 10 faster events from the OMNI website (http://cdaweb.gsfc.nasa.gov/istp_public/) and from the Proton Monitor (PM) on board SOHO mission (http://umtof.umd.edu/pm/). For each event, we have found the shock onset date, time, shock speed and transit time as described below. The shocks are identified using sudden discontinuity in plasma parameters of proton density, flow speed and proton temperature. The shock speeds (see e.g., Douglas and Park, 1983) are calculated using density and speed from upstream and downstream of shock, $Vs = (v_1 n_1 - v_2 n_2)/(n_1 - n_2)$, v_1 and n_1 are speed and density before the shock front (upstream region), v_2 and n_2 are the speed and density after the shock front (downstream region). Transit time is calculated by the time difference between the CME time in LASCO C2 image and shock time in WIND spacecraft data. The faster 10 CMEs and their associated interplanetary parameters are listed in Table 1. The IP shock arrival date to 1 AU (yymmdd format), time and speed are listed in the first three columns of Table 1. The strength of the shocks is identified by using Alfvenic Mach numbers (M_a) and magnetosonic Mach numbers (M_s), shock transit times are listed in column 4–6 in Table 1. ICME arrival date to 1 AU, time and speed are listed in the column 7–9 and the corresponding white-light CME's date, time, type (Halo or partial Halo), plane-of-sky speed, and acceleration are listed in the column 10–14 of Table 1.

3. Results and discussion

Fig. 1 shows the histograms of (a) initial speeds of CMEs (V_{INT}) in the LASCO field of view (FOV), (b)

Table 1
List of IP shocks, ICMEs and associated CMEs.

| No. | IP shock | | | | | | ICME | | | CME | | | | | |
	Date	Time	Speed	M_a	M_s	TT	Date	Time	Speed	Date	Time	H/P	Location	Speed	Acceleration
	yymmdd	hhmm	km s^{-1}			h	yymmdd	hhmm	km s^{-1}	yymmdd	hhmm			km s^{-1}	m s^{-2}
01	031104	0610	0875	4.7	5.5	36.7	031104	0900	750	031102	1730	H	S14W56	2598	−32.4
02	031106	1940	0633	4.3	4.7	47.8	031106	2010	600	031104	1954	H	S19W83	2657	434.8
03	041111	1600	0584	6.5	6.6	37.6	041112	0000	690	041110	0226	H	09W49	3387	−108
04	050117	0800	0900	7.3	10.1	32.9	050117	1200	800	050115	2306	H	N15W05	2861	−127.4
05	050118	1800	0887	5.6	5.9	32.1	050118	2100	990	050117	0954	H	N15W25	2547	−159.1
06	010404	1500	0772	3.7	4.2	40.9	010404	1730	790	010402	2206	P	N19W72	2505	108.5
07	010925	2017	0631	4.5	4.8	33.8	010926	0200	550	010924	1030	H	S16E23	2402	54.1
08	020423	0500	0660	4.9	5.6	51.6	020423	0900	550	020421	0127	H	S14W84	2393	1.4
09	050824	0600	0590	5.0	5.4	36.5	050824	0940	630	050822	1730	H	S13W65	2378	108
10	990606	0950	0512	7.8	9.5	50.4	990606	1100	435	990604	0725	P	N17W69	2230	5.6
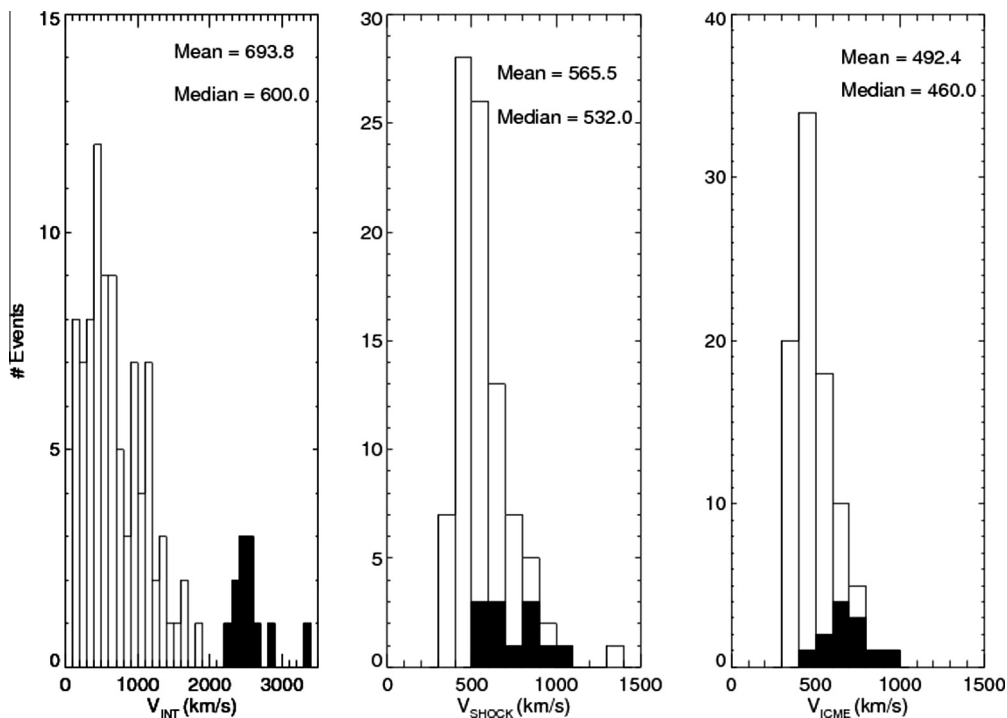
Fig. 1. Histograms of (a) initial speed (V_{INT}) in the LASCO field of view, (b) speed of the associated interplanetary shock at 1 AU (V_{SHOCK}), and (c) speed of the CME at 1 AU (V_{ICME}). The grid line indicates the faster 10 CME events. Each bin size is 100 km/s.

in situ speeds of their corresponding interplanetary shocks (V_{SHOCK}) and (c) interplanetary CMEs at 1 AU (V_{ICME}). V_{INT} is the projected speed as it appears on the plane of the sky. Since the majority of the CME originate from disk-center, the projection effects may be quite large. It is evident from the histograms that at 1 AU, the speed range of ICMEs and IP shocks tends to narrow towards the ambient solar wind (i.e., speed ~500 km/s) (see, e.g., Gopalswamy et al. (2001); Cane and Richardson, 2003). It is clearly seen that the wide range of speeds in the LASCO FOV i.e., ~100–3400 km/s tends to narrow to a range of ~400–1000 km/s at the near-Earth region in the cases of the shock and CME. Wang and Sheeley (1994), Webb et al., 2009; Manoharan and Mujiber Rahman (2011), suggest that, (i) the slowing down of events is due

to the drag term (Cargill, 2004; Vršnak et al., 2004; Vršnak and Žic 2007; Vršnak et al., 2010) or (ii) a snow plow (Tappin, 2006). The CME speeds vary from 136 km/s to 3500 km/s with a mean value of 694 km/s and the median value of 600 km/s. On the other hand, the IP shock speed values vary from ~400 km/s to 1400 km/s with a mean and median value of 565 km/s and 532 km/s, respectively. Similarly, ICME speed ranges from 400 km/s to 1000 km/s with a mean value of 492 km/s (median value = 460 km/s). Since the CME speed, ICME speed and IP shock speed distributions are not symmetric, we have also given the median values. From this analysis, it is noted that the IP shock speed is slightly greater than the ICME speed. Hence, it is evident that the IP shock reaches 1 AU faster than the ICME. This is obvious since

the shocks are driven by the ICMEs. The group of 10 faster CMEs ($V_{INT} > 2200$ km/s) is clearly seen in Fig. 1 (as shown in shaded area), whereas their IP shock (V_{SHOCK}) and ICME (V_{ICME}) speeds are also seen in the figure in the higher speed range. Their speeds are reduced to 500–1000 km/s due to the exchange of energy between the CME and the ambient solar wind medium (see, e.g., Manoharan, 2006).

From the correlation plot (Fig. 2), between ICME speed and IP shock speed, we note that they are linearly well correlated and the correlation coefficient obtained is $R^2 = 0.84$, i.e., as the ICME speed increases, there is an increase of IP shock speed. It denotes that both ICME and IP shock speeds depend on each other (Manoharan et al., 2004). Siscoe and Odstrcil (2008) developed a rigorous understanding of the relationship between shock speed and properties of the CME including size, speed and expansion rate. In Fig. 2, the dotted line indicates the events with equal values of ICME and IP shock speed. It is noted that, almost all the events lie below the dotted line for which $V_{ICME} < V_{SHOCK}$ and only very few events lie on the dotted line for which $V_{ICME} = V_{SHOCK}$. It is also worth pointing out that 8 of the 10 fastest CMEs are "above" the trend line and four have $V_{ICME} > V_{SHOCK}$. When we further investigated the four events having $V_{ICME} > V_{SHOCK}$, it is seen that the differences in IP shock and ICME speeds of these events are 106 km/s, 103 km/s, 18 km/s, 40 km/s. They are within the range 18–106 km/s. This range lies within the uncertainty in the measurement of ICME speeds (Temmer et al., 2011) consistent with a value of $V_{ICME} = V_{SHOCK}$.

Fig. 3 (left panel), shows the distributions of travel time plotted against number of events. The travel time of a CME to the Earth is an indicator of its typical average speed between LASCO FOV and the Earth (see, e.g., Manoharan and Mujiber Rahman, 2011). From this figure, we observe that a large number of events have travel time in the range 40–80 h. The mean and median values of travel time are nearly 62 h. On the other hand, the faster events for which $V_{INT} > 2200$ km/s are seen in the 40–60 h range
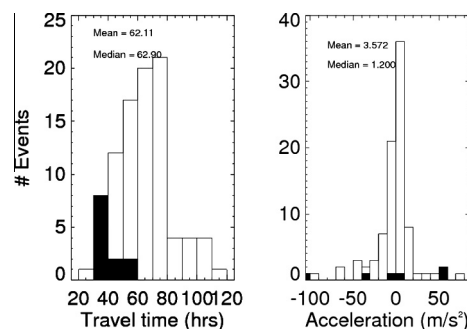
Fig. 3. Distribution diagrams of travel time and acceleration. The shaded area indicates the faster 10 CME events ($V_{INT} > 2200$ km/s). The bin size is 10 h in travel time and 10 m/s^2 in acceleration. The highly accelerated or decelerated events are not shown in the acceleration plot (right side panel).

with a mean travel time of 40 h (shown as shaded area in Fig. 3).

Fig. 3 (right panel), shows the distribution diagram of acceleration of all 101 events in the LASCO FOV. From this figure, we note that a large number of events tend to be in the acceleration range of -10 m/s^2 to 10 m/s^2 and a considerable number of events (35 out of 101) shows nearly zero acceleration between -5 m/s^2 and 5 m/s^2. However, among the 10 faster CME events ($V_{INT} > 2200$ km/s), equal number of events are accelerated and decelerated with acceleration range -159 m/s^2 to 434 m/s^2. The faster events are indicated as shaded area in the distribution diagrams. Among the 101 events, only five events have less than three data points. They are, 970917 ($a = 0$ m/s^2), 971119 ($a = -5$ m/s^2), 031102 ($a = -32$ m/s^2), 031104 ($a = 434$ m/s^2), 990604 ($a = 5.6$ m/s^2). The acceleration of only one event is very high and these events are not included for our further analysis.

Earlier studies have presented the dependency of transit time on CME speed. In our present study, we have tried to see the correlation between the ICME/IP shock speeds and the transit time (Fig. 4a and b). It looks like, for a given transit time, ICME and shock properties at 1 AU are slower than expected from the fitted straight line. All the fast events ($V_{INT} > 2200$ km/s) are below the fitted line, i.e., their ICME and shock properties are lower than the fitted line on ICME/IP shock speed versus transit time. Maybe this indicates something about where the decelerations mostly happen. Many events reaching faster than the transit time predicted by the straight line imply that the deceleration of these events occurs at larger distances or their speed become similar to the ambient speed beyond 1 AU. A thin line drawn on this plot shows the line of constant speed events. Almost all of the events lie below this constant speed line, which proves that they are subjected to an aerodynamic drag force or a snow plow effect (note that the inherent magnetic force is thought to be a driving mechanism which should put these events above the constant line not below).

In this connection a new plot between CME speed and transit time is drawn as shown in Fig. 4c. The arrival time
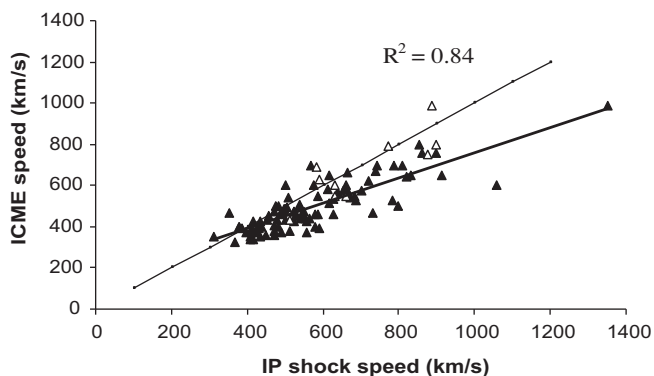

Fig. 2. Interplanetary CME speed is correlated with IP shock speed. The symbol Δ refers to the faster CME events and we note that most of the faster events lie above the correlation line. The dotted line indicates that the events for which $V_{ICME} = V_{SHOCK}$.

(a)

$y = -0.0732x + 106.57$
$R^2 = 0.4277$

Transit time (hours) vs IP shock speed (km/s)

(b)

$y = -0.1037x + 115.98$
$R^2 = 0.4573$

Transit time (hours) vs ICME speed (km/s)

(c)

$y = -0.0186x + 79.151$
$R^2 = 0.4774$
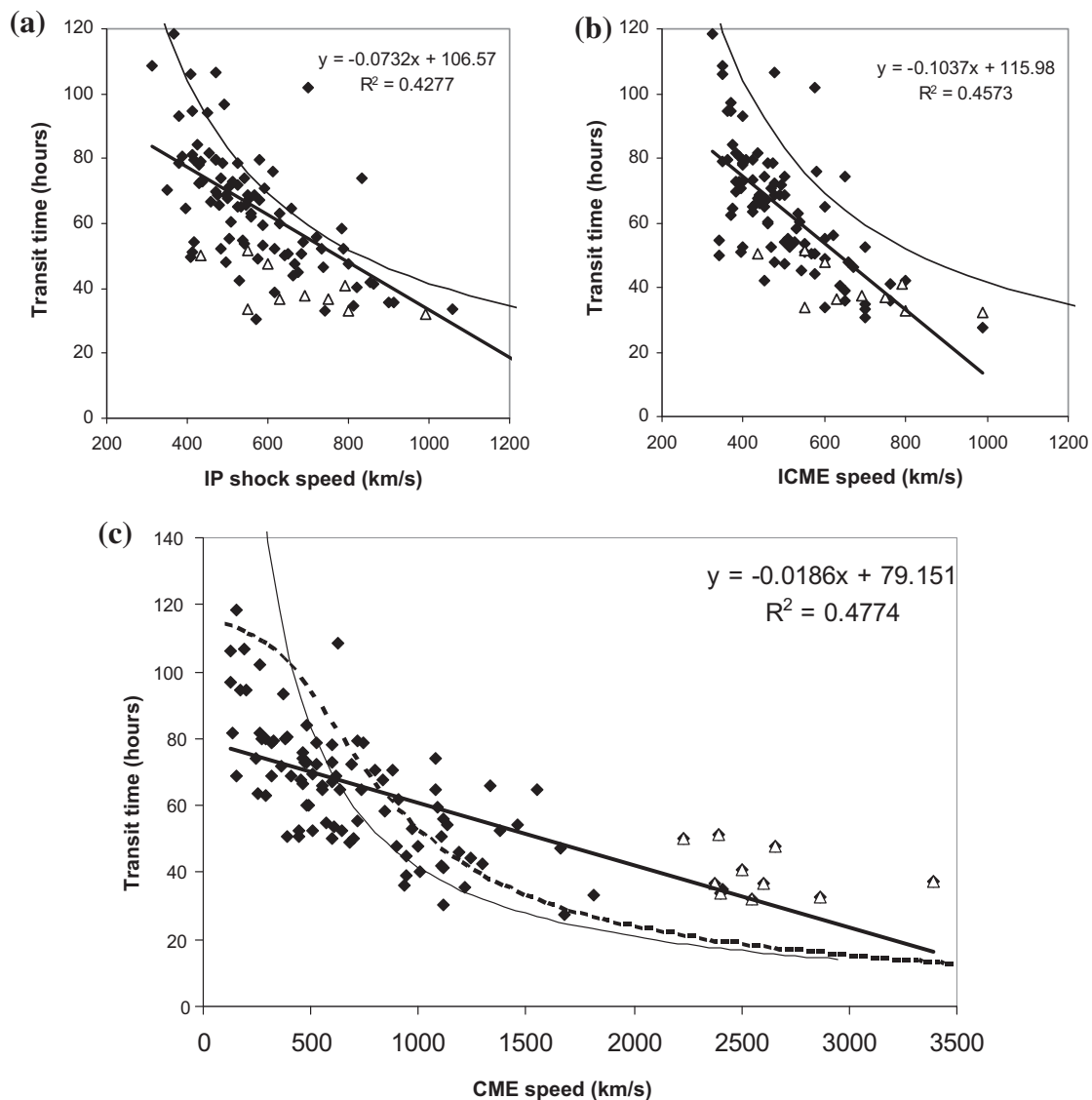
Transit time (hours) vs CME speed (km/s)

Fig. 4. Transit time to arrival of CME to 1 AU is plotted against the speeds of (a) Interplanetary shock and (b) Interplanetary CME. (The symbol Δ indicates the faster CME events).

of faster events are compared with the normal events in this figure. Thin line shows the transit time of events travel with constant-speed and dashed-line shows the transit time according to the empirical shock arrival (ESA) model of Gopalswamy et al. (2005) for an acceleration cessation distance of 0.7 AU. It seems that at high speeds (>2000 km/s), the ESA curve predicts only a slight excess of 3–1 h with that of constant-speed curve for 2000–3000 km/s. But, observations show that all the faster events have higher transit time (14–30 h) than the predicted times of both ESA and constant-speed curves. The deviation of slow and fast events from the ESA curve is similar to the results already reported by Manoharan et al. (2004) and Kim et al. (2007). A straight line is also fitted on all the data points including the faster events. It shows a correlation coefficient of 0.69 between the CME speed and transit time.

Fig. 5a, shows the correlation plot between CME speed measured in the LASCO FOV and IP shock speed mea-

sured at 1 AU from the spacecraft data. From the figure, it is evident that large number of events are scattered in the CME speed range of ~100 km/s to ~1500 km/s for an IP shock speed range ~350 km/s to 700 km/s. Also, we note that a large scattering in IP shock speeds for a given CME speed. The correlation coefficient obtained for this plot is $R^2 = 0.59$. Similar to this, there is a weak correlation (correlation coefficient, $R^2 = 0.52$) between ICME speed and CME speed (Fig. 5b). The faster CME events are seen separately at the right end of the distribution. The linear relation obtained between CME speed and ICME speed $V_{ICME} = 396.4 + 0.136 \ V_{CME}$, is more or less similar to that of Lindsay et al. (1999) and Gopalswamy et al. (2001). A slight deviation can be noted for the faster events from the trend of Lindsay et al. (1999). From Fig. 5a, it can be noted that most of the faster events have slower IP shock speed because of heavy deceleration. In both the plots, the dashed line indicates the zero accelera-
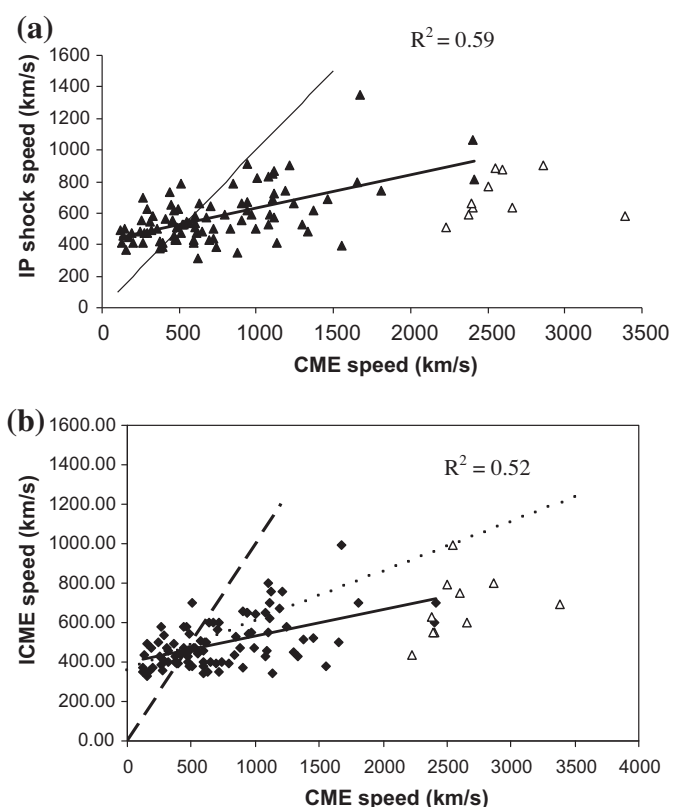
Fig. 5. CME speed is plotted against (a) IP shock speed and (b) ICME speed. Dashed line indicates zero acceleration line. The events which are left side of the dashed line are accelerated and the events on the right side are decelerated. (The symbol Δ indicates the faster CME events). The solid line denotes the linear fit to the normal events. Dashed line denotes zero acceleration line. The dotted line shows the trend obtained by Lindsay et al. (1999).

tion for which the CME speed is equal to IP shock/ICME speeds. But, it is seen that there are no events along this zero acceleration line. Most of the events lie on the right side of the zero acceleration line which indicates that all of them are decelerated in the interplanetary medium. There are a few events having low initial CME speed ($V_{INT} < 400$ km/s) on the left side of the zero acceleration line are accelerated in the interplanetary medium to adjust to the ambient solar wind speed.

Sheeley et al. (1985) found the slow speed (<200–300 km/s) solar wind at a height range in the corona 2.5–10 $R_{\odot}$ could be linked to ICME-related interplanetary shocks at heliocentric distances of 0.3–1.0 AU. These observations implied that slow CMEs can be accelerated in the high corona or in the inner heliosphere to speeds higher than the ambient solar wind speed or may produce ICMEs expanding at supermagnetosonic speeds. On the other hand the fast CMEs can be decelerated in the interplanetary medium by the aerodynamical drag (i.e., solar wind drag) and adjusted to the speed of the ambient medium (Gopalswamy et al., 2001). The weak correlations in the plots (Fig. 5a and 5b), confirms the effect of drag force due to solar wind on the CME propagation in the inter-

planetary medium (see, e.g., Sheeley et al., 1985; Vršnak et al., 2001, 2004; Manoharan, 2006; Shanmugaraju et al., 2009; Manoharan and Mujiber Rahman, 2011).

Fig. 6, shows the acceleration of CME determined in the LASCO FOV against IP shock speed and ICME speed measured at 1 AU from the spacecraft data. There is no correlation between IP shock speeds and acceleration. It may be because there are nearly equal numbers of accelerating and decelerating events. However, from the correlation plots, we note the faster ICMEs/IP shocks decelerating/accelerating more than the slow speed events (see, e.g., Wang and Sheeley, 1994).

As shown in Fig. 7, the faster events having travel time around 40 h seem to be heavily accelerated or decelerated in the LASCO FOV. Finally, we classify 101 events into two groups, (i) $V_{CME} > V_{ICME}$ and (ii) $V_{CME} < V_{ICME}$ having number of events 70 and 31, respectively. The first group implies that those events are decelerated, while the second group events are accelerated in the interplanetary medium. We have also checked the acceleration values of these two groups of events in the LASCO FOV and found that many of the first and second groups of events have $a < 0$ and $a > 0$, respectively. The number of events in the first group of decelerating events is twice the number of events in accelerating group. Hirshberg et al. (1987), Burlaga et al. (1987) and Gosling et al. (1987) recognized that the solar wind stream structure could alter an ICME in transit by adding to its compression and reorienting both the internal and surrounding flows and fields. Iju et al. (2011) suggested the deceleration of fast ICMEs and acceleration of slow ICMEs and converge to the background solar wind speed. Also, they pointed out that both the acceleration and deceleration stop around 0.8 AU with a speed of 490 km/s. These results as well as the results we discuss below in the present study, support a hypothesis that the radial motion of ICME is governed by drag force caused by an interaction with the background solar wind. Also, we have found that equal number of accelerating and decelerating CMEs among the fast group of 10 events with initial CME speed (>2200 km/s).

A summary of all the kinematic properties (mean and standard deviation) of CMEs, ICMEs and IP shocks are given in Table 2. The mean and standard deviation values of 91 normal and 10 faster CMEs are compared in this table. We find that the mean speeds are higher for the faster 10 events than the 91 normal ones. In the LASCO field of view, the residual acceleration is found to be more negative for these faster events. Correspondingly, it can be seen that the faster events are decelerated more in the interplanetary medium. On the other hand, the travel time, standoff time and standoff distance are lesser for faster events. In contrast to this, the shock strength inferred from the Mach number is greater for faster events.

The interplanetary propagation of CMEs is examined by the interplanetary acceleration for 101 CME events, which is calculated using the ratio of difference of ICME speed with CME speed (Δv) and travel time of CME to
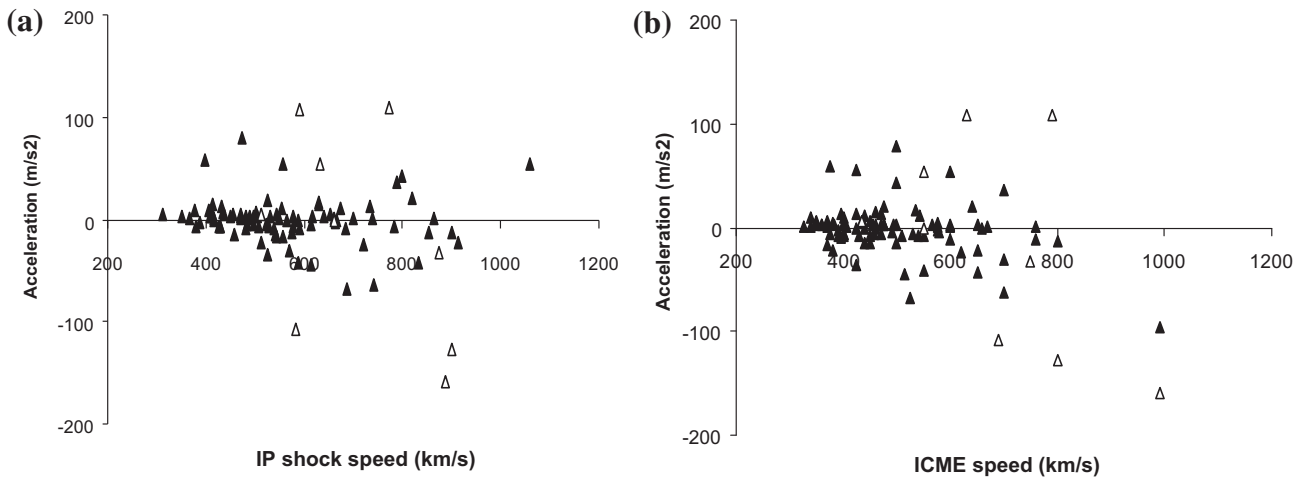
Fig. 6. Acceleration of CME is plotted against (a) IP shock and (b) ICME speeds. (The symbol Δ indicates the faster CME events).
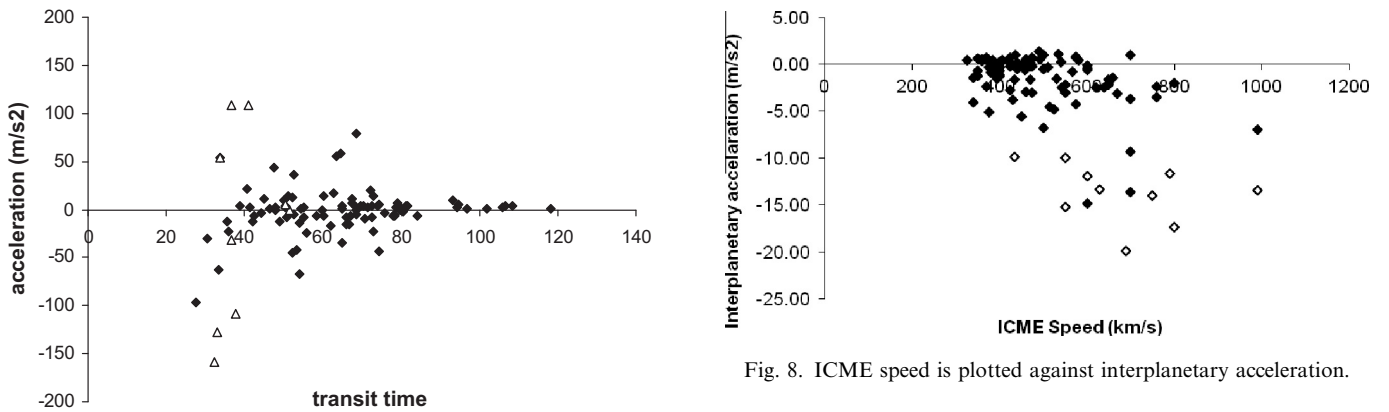

Fig. 7. Acceleration of CME events in LASCO field of view are plotted against CME transit time to 1 AU. (The symbol Δ indicates the faster CME events).

Fig. 8. ICME speed is plotted against interplanetary acceleration.

1 AU. Fig. 8, shows the correlation of interplanetary acceleration with ICME speed. The faster 10 events have more negative acceleration than the normal 91 CMEs. Further, we note that most of the normal events lie around zero acceleration. The events with positive interplanetary acceleration are slow speed normal events. The relation between ICME speed and IP acceleration $a = -0.0181$ $(V_{ICME} - 365)$, is slightly different from $a = -0.0054$ $(V_{CME} - 406)$. There is a significant difference in the coefficient of these two equations (more than a factor of three). The difference may be related to the fact that while we obtained the relation between interplanetary acceleration and ICME speed, the relation of Gopalswamy et al. (2001) was derived between interplanetary acceleration and CME speed.

The mean and standard deviation values of interplanetary acceleration for normal events is -1.49 m/s^2 and 2.77 m/s^2, respectively. However, for the faster events the values are -13.67 m/s^2 and 3.18 m/s^2, respectively as shown in Table 2. As we described already ICMEs are

Table 2
Average values and standard deviation values of CME speed, ICME speed, IP shock speed, standoff time (SOT), standoff distance (SOD), Alfvenic Mach number (M_a), magnetosonic Mach number (M_s) and Transit time (TT) of normal events and faster 10 events.

Properties		CME		IP shock				ICME			
	Speed	Acceleration	Speed	M_a	M_s	TT	Speed	SOT	SOD	IP Acceleration
	km s^{-1}	m s^{-2}	km s^{-1}			h	km s^{-1}	h	R_{Sun}	m s^{-2}
(i) Normal events										
Mean	731.54	0.92	573.66	2.94	2.44	64.55	495.95	11.63	29.40	−1.49
Stdev	469.01	32.75	168.01	1.85	1.39	18.82	122.71	5.22	14.45	2.77
(ii) Faster events										
Mean	2595.80	−17.90	704.40	5.43	6.23	40.03	678.50	3.55	12.58	−13.67
Stdev	328.40	113.53	142.34	1.35	2.00	7.34	159.97	2.14	7.57	3.18

accelerated/decelerated as a result of the ICME-solar wind interaction, e.g., due to drag forces between the ICME and the solar wind environment (e.g., Vršnak and Gopalswamy, 2002).

In Fig. 9, we have correlated the interplanetary acceleration with CME acceleration obtained from SOHO/LASCO CME catalog. Out of the 10 faster CME events, five events show negative acceleration and two events in the zero acceleration region. The remaining three events are in the postive acceleration region. Most of the normal 91 events are concentrated in the zero acceleration regions. That implies, most of the events are adjusted to the solar wind with the Sun–Earth distance (Iju et al., 2011). The mean and standard deviation values for CME acceleration in LASCO FOV of normal events are $0.92 \, \text{m/s}^2$ and $32.75 \, \text{m/s}^2$, respectively, whereas for the faster events the values are $-17.9 \, \text{m/s}^2$ and $113.53 \, \text{m/s}^2$, respectively (refer Table 2). It should be noted that the events having positive acceleration in the LASCO FOV have negative acceleration in the interplanetary medium.

In Fig. 10, we have correlated the interplanetary acceleration with CME speed and it is interesting to note that both parameters are highly correlated. Most of the faster CMEs show the higher negative acceleration than the normal ones. Further, we note that many normal events are concentrated in the region $-5 \, \text{m/s}^2$ to $+2 \, \text{m/s}^2$ i.e., the faster events undergo higher deceleration upto Earth and even beyond the Earth distance. The relation between CME speed and IP acceleration is: $a = -0.0062 \, (V_{\text{CME}} - 485)$ which is similar to $a = -0.0054 \, (V_{\text{CME}} - 406)$ of Gopalswamy et al. (2001) obtained for 59 CME – MC pairs. But for the faster events, a slight deviation can be seen in the figure.

The interplanetary acceleration is plotted against travel time of CMEs in Fig. 11 as studied already in Manoharan and Mujiber Rahman (2011), more events adjust to the solar wind and travel with nearly net zero acceleration within the 1 AU distance. However, it is seen that the faster events with less travel time (around 20–40 h) face higher negative acceleration $(>-10 \, \text{m/s}^2)$ in the interplanetary medium up to 1 AU and they may adjust to solar wind speed beyond 1 AU. One can distinguish between a deceleration proportional to the CME speed minus solar wind speed or quadratic (drag). When we further looked into
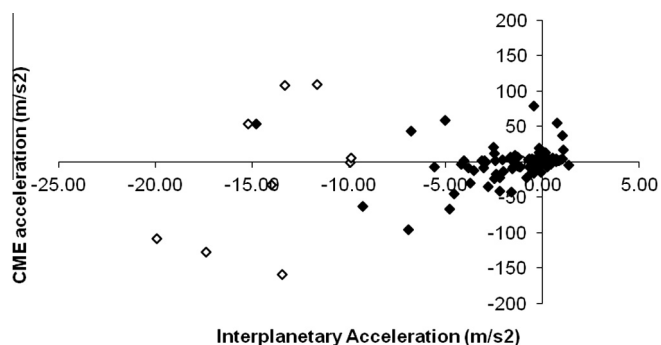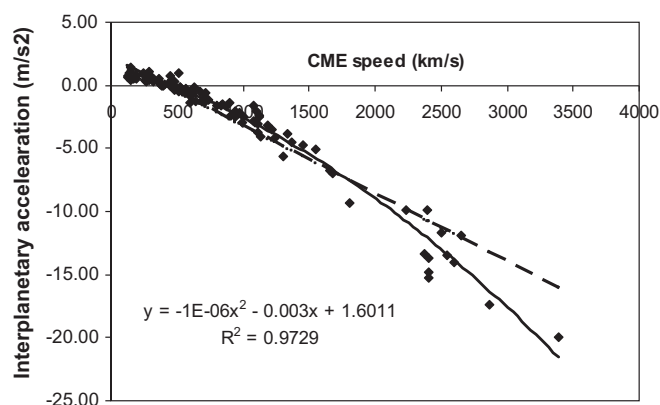

Fig. 10. Correlation of interplanetary acceleration with CME speed. The straight line shows the quadratic fit the 101 data points. The dashed line shows trend obtained by Gopalswamy et al. (2001).
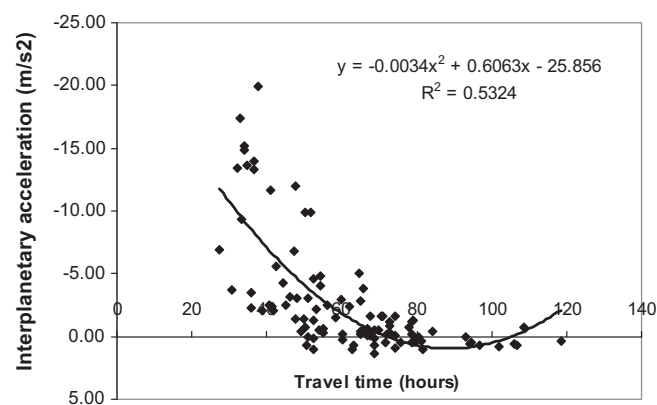

Fig. 11. Correlation of the interplanetary acceleration against the travel time of CMEs.

the Fig. 11 regarding this case, it is seen that $R^2 = 0.4$ for linear and $R^2 = 0.53$ for quadratic. Hence a quadratic is a bit better but well within the uncertainty of the fit.

4. Summary

In the present study, we have analyzed a set of 101 earth-directed CME events listed in Manoharan et al. (2004) and Mujiber Rahman et al. (2012). This list of halo and partial halo CMEs provides a sample of disc centered events, covering a wide range of speeds ($\sim$140–3200 km/s) in the LASCO FOV. Mainly a group of 10 faster CMEs ($V_{\text{INT}} > 2200$ km/s) is compared with 91 normal CMEs. Each event's interplanetary shock and ICME data obtained by near-Earth spacecraft are considered to study the properties of CMEs in the interplanetary medium. From the distribution diagrams of CME, ICME and IP shock speeds, we note that a large number of events tends to narrow towards the ambient solar wind speed (i.e., $\sim$500 km/s). Also, we find that the IP shock speed and the average ICME speed measured at 1 AU are well linearly correlated (correlation coefficient, $R^2 = 0.84$) confirm-

Fig. 9. Interplanetary acceleration is plotted against CME acceleration.

ing their close association and earlier results. However, the mean value of interplanetary shock speed is found to be slightly higher than that of ICMEs. Most events show IP shock/ICME travel time in the range of ~40–80 h which is consistent with the literature values. It is found that the faster CMEs ($V > 2200$ km/s) have the lower transit time (<50 h) than the normal CMEs. The correlation plots between IP shock/ICME speed and transit time show their dependency on each other. In addition, the weak correlations between IP shock/ICME speeds with CME speed demonstrate the effect of drag force by the solar wind. Especially, we have examined the interplanetary propagation of normal and faster CMEs using their acceleration values near the Sun (in the LASCO FOV) and interplanetary acceleration. From the correlation of acceleration of CMEs (in LASCO FOV) with interplanetary parameters, we find that considerable number of events show nearly zero acceleration which implies that fast moving ICMEs decelerate heavily and slow ICMEs gradually tend to equal to the ambient (i.e., background) solar wind as suggested by Manoharan (2006). In addition, we find that among 101 events, there are nearly equal numbers of events having positive and negative acceleration in the LASCO FOV. Whereas, there are 70% of events found to be decelerated but only 30% of events are found to be accelerated in the interplanetary medium. The relation between CME speed and IP acceleration is similar to that of Lindsay et al. (1999) and Gopalswamy et al. (2001) except slight deviation for faster events. It is also seen that the faster events with less travel time face higher negative acceleration (> -10 m/s^2) in the interplanetary medium up to 1 AU. Also, the mean values of all the kinematic properties of normal and faster events show significant changes.

Acknowledgement

References

Balogh, A., Magnetic fields in the heliosphere at solar minimum and solar maximum. In: ASP Conference Proceedings, vol. 269, Astronomical Society of the Pacific, pp. 37–46, 2002.

Burlaga, L.F., Behannon, K.W., Klein, L.W.J. Compound streams, magnetic clouds, and major geomagnetic storms. Geophys. Res. 92, 5725–5734, 1987.

Burlaga, L.F.. Interplanetary Magnetohydrodynamics, International Series in Astronomy and Astrophysics, 3. Oxford University Press, 1995.

Cane, H.V., Richardson, I.G. Interplanetary coronal mass ejections in the near-Earth solar wind during 1996–2002. J. Geophys. Res. 108, 1156, 2003.

Cargill, Peter J. On the aerodynamic drag force acting on interplanetary coronal mass ejections. Sol. Phys. 221, 135–149, 2004.

Case, A.W., Spence, H.E., Owens, M.J., Riley, P., Odstrcil, D. Ambient solar wind's effect on ICME transit times. Geophys. Res. Lett. 35, L15105, 2008.

Chen, J. Theory of prominence eruption and propagation: interplanetary consequences. J. Geophys. Res. 101, 27499–27520, 1996.

Corona-Romero, P., Gonzalez-Esparza, A. Deceleration of CMEs in the interplanetary medium: comparison of different analytic models, in: American Geophysical Union, Fall Meeting 2011, abstract #SH23A-1945, 2011.

Douglas, W.P., Park, G.K. Upstream electron oscillations and ion overshoot at an interplanetary shock wave. Geophys. Res. Lett. 10, 529–532, 1983.

Gosling, J.T. Coronal mass ejections – the link between solar and geomagnetic activity. Phys. Fluids B 5, 2638–2645, 1993.

Gosling, J.T., Thomsen, M.F., Bame, S.J., Zwickl, R.D. The eastward deflection of fast coronal mass ejecta in interplanetary space. J. Geophys. Res. 92, 12399–12406, 1987.

Gopalswamy, N., Lara, A., Yashiro, S., Kaiser, M.L., Howard, R.A. Predicting the 1-AU arrival times of coronal mass ejections. J. Geophys. Res. 106, 29207–29218, 2001.

Gopalswamy, N., Lara, A., Manoharan, P.K., Howard, R.A. An empirical model to predict the 1-AU arrival of interplanetary shocks. Adv. Space. Res. 36, 2289–2294, 2005.

Gopalswamy, N., Thompson, W.T., Davila, J.M., Kaiser, M.L., Yashiro, S., Mäkelä, P., et al. Relation between type II bursts and CMEs inferred from STEREO observations. Sol. Phys. 259, 227–254, 2009.

Hirshberg, J., Nakagawa, Y., Wellck, R.E. Propagation of sudden disturbances through a non-homogeneous solar wind. J. Geophys. Res 79, 3726–3730, 1987.

Howard, T.A., Fry, C.D., Johnston, J.C., Webb, D.F. On the evolution of coronal mass ejections in the interplanetary medium. Astrophys. J. 667, 610–625, 2007.

Iju, T., Tokumaru, M., Fujiki, K., Kinematical properties of interplanetary coronal mass ejections detected by interplanetary scintillation observations during the solar cycle 23, in: American Geophysical Union, Fall Meeting, abstract SH23A-1939, 2011.

Jian, L., Russell, C.T., Luhmann, J.G., Skoug, R.M. Evolution of solar wind structures from 0.72 AU to 1 AU. Adv. Space Res. 41, 259–266, 2008.

Kim, K.-H., Moon, Y.-J., Cho, K.-S. Prediction of the 1-AU arrival times of CME-associated interplanetary shocks: Evaluation of an empirical interplanetary shock propagation model. J. Geophys. Res. 112, A05104, 2007.

Lindsay, G.M., Luhmann, J.G., Russell, C.T., Gosling, J.T. Relationships between coronal mass ejection speeds from coronagraph images and interplanetary characteristics of associated interplanetary coronal mass ejections. J. Geophys. Res. 104, 12515–12524, 1999.

Lugaz, N., Manchester IV, W.B., Gombosi, T.I. Numerical simulation of the interaction of two coronal mass ejections from Sun to Earth. Astrophys. J. 634, 651–662, 2005.

Lugaz, N., Roussev, I.I. Numerical modeling of interplanetary coronal mass ejections and comparison with heliospheric images. J. Atm. Sol. Terr. Phys. 73, 1187–1200, 2011.

Maloney, Shane.A., Gallagher, Peter.T. Solar wind drag and the kinematics of interplanetary coronal mass ejections. Astrophys. J. Lett. 724, L127–L132, 2010.

Manoharan, P.K., Gopalswamy, N., Yashiro, S., Lara, A., Michalek, G., Howard, R.A. Influence of coronal mass ejection on propagation of interplanetary Shocks. J. Geophys. Res. 109, A06109, 2004.

Manoharan, P.K. Evolution of coronal mass ejections in the inner heliosphere: a study using white-light and scintillation images. Sol. Phys. 235, 345–368, 2006.

Manoharan, P.K., Mujiber Rahman, A. Coronal mass ejections propagation time and associated internal energy. J. Atmos. Sol. Terr. Phys. 73, 671–677, 2011.

Mujiber Rahman, A., Umapathy, S., Shanmugaraju, A., Moon, Y.J. Solar and interplanetary parameters of CMEs with and without type II radio bursts. Adv. Space Res. 50, 516–525, 2012.

Shanmugaraju, A., Moon, Y.-J., Vršnak, B., Vrbanec, D. Radial evolution of well-observed slow CMEs in the distance range 2–30 $R_\odot$. Sol. Phys. 257, 351–361, 2009.

Sheeley Jr., N.R., Sheeley Jr., N.R., Howard, R.A., Michels, D.J., Koomen, M.J., et al. Coronal mass ejections and interplanetary shocks. J. Geophys. Res. 90, 163–175, 1985.

Siscoe, G., Odstrcil, D. Ways in which ICME sheaths differ from magnetosheaths. J. Geophys. Res. 113, A9, 2008.

Tappin, S.J. The deceleration of an interplanetary transient from the Sun to 5 Au. Sol. Phys. 233, 233–248, 2006.

Temmer, M., Rollett, T., Möstl, C., Veronig, A., Vršnak, B., Odstrčil, D. Influence of the ambient solar wind flow on the propagation behavior of interplanetary coronal mass ejections. Astrophys. J. 743, 12, 2011.

Vršnak, B., Aurass, H., Magdalenić, J., Gopalswamy, N. Band-splitting of coronal and interplanetary type II bursts. I. Basic properties. Astron. Astrophys. 377, 321–329, 2001.

Vršnak, B., Gopalswamy, N. Influence of the aerodynamic drag on the motion of interplanetary ejecta. J. Geophys. Res. 107, 1019, 2002.

Vršnak, B., Ruždjak, D., Sudar, D., Gopalswamy, N. Kinematics of coronal mass ejections between 2 and 30 solar radii. What can be learned about forces governing the eruption? Astron. Astrophys. 423, 717–728, 2004.

Vršnak, B., Žic, T. Transit times of interplanetary coronal mass ejections and the solar wind speed. Astron. Astrophys. 472, 937–943, 2007.

Vršnak, B., Žic, T., Falkenberg, T.V., Möstl, C., Vennerstrom, S., Vrbanec, D. The role of aerodynamic drag in propagation of interplanetary coronal mass ejections. Astron. Astrophys. 512, A43, 2010.

Wang, Y.-M., Sheeley Jr., N.R. Global evolution of interplanetary sector structure, coronal holes, and solar wind streams during 1976–1993: stackplot displays based on solar magnetic observations. J. Geophys. Res. 99 (A4), 6597–6608, 1994.

Webb, D.F., Howard, T.A., Fry, C.D., Kuchar, T.A., Odstrcil, D., Jackson, B.V., et al. Study of CME propagation in the inner heliosphere: SOHO LASCO, SMEI and STEREO HI observations of the January 2007 events. Sol. Phys. 256, 239–267, 2009.

Yashiro, S., Gopalswamy, N., Michalek, G., St. Cyr, O.C., Plunkett, S.P., Rich, N.B., Howard, R.A.A. Catalog of white light coronal mass ejections observed by the SOHO spacecraft. J. Geophys. Res. 109, A07105, 2004.